Significant West Antarctic Cooling in the Past Two Decades Driven by Tropical Pacific Forcing

Xueying Zhang, Yetang Wang⊙, Shugui Hou, and Petra Heil

ABSTRACT: During the second half of the twentieth century, the West Antarctic Ice Sheet (WAIS) has undergone significant warming at more than twice the global mean and thus is regarded as one of the most rapidly warming regions on Earth. However, a reversal of this trend was observed in the 1990s, resulting in regional cooling. In particular, during 1999–2018, the observed annual average surface air temperature had decreased at a statistically significant rate, with the strongest cooling in austral spring. The spring cooling correlates significantly with the second leading modes (EOF2) derived from empirical orthogonal function (EOF) analysis on the sea level pressure over Antarctica during 1999–2018, associated with the negative phase of the interdecadal Pacific oscillation with an average of cooling of central and eastern tropical Pacific surface sea temperature (SST) anomalies. The EOF2 results in the enhanced cold southerly winds on the continental WAIS through the cyclonic conditions over the Amundsen Sea region and a blocking high in the Drake Passage and northern Antarctic Peninsula, causing the WAIS cooling trend.

KEYWORDS: Antarctica; Atmospheric circulation; Ice sheets; Teleconnections

AFFILIATIONS: **Zhang and Wang**—College of Geography and Environment, Shandong Normal University, Jinan, China; **Hou**—School of Oceanography, Shanghai Jiao Tong University, Shanghai, China; **Heil**—Australian Antarctic Division, Kingston, and Australian Antarctic Program Partnership, University of Tasmania, Hobart, Tasmania, Australia

As one of nine tipping elements of the Earth system (Schellnhuber 2009; Lenton 2021), the West Antarctic Ice Sheet (WAIS) is losing mass at an accelerated rate, with a cumulatively contribution to the global sea level rise of 6.9 ± 0.6 mm since the late 1970s (Rignot et al. 2019). Regional climate change may exert considerable impact on the glacial ice dynamics (e.g., basal melting mediation via Ekman transport) (Kimura et al. 2017) and ice sheet mass balance (e.g., accumulation from precipitation and snow drift; surface melting via warming air temperature), raising concern about flow-on effects. Since 1958, the WAIS experienced significant warming (Steig et al. 2009) with the warming rate of more than doubling the global mean for the second half of the twentieth century. Hence, the WAIS is one of the most rapidly warming regions on Earth (Bromwich et al. 2013, 2014). However, over the early twenty-first century, warming over the Antarctic Peninsula transfers to the cooling trends (Turner et al. 2016). Jones et al. (2019) reported the seasonal and annual cooling during 1998–2016 over Byrd Station. Clem et al. (2020) showed that the warming of the South Pole from 1989 to 2018 is accompanied by cooling in Antarctic Peninsula and West Antarctica.

Much attention has been paid to the contribution of the El Niño–Southern Oscillation (ENSO) to Antarctic climate changes. Recent studies have shown that central tropical Pacific forcing between the 1950s and the 2000s was largely responsible for the rapid winter warming in West Antarctica via atmospheric teleconnections through an atmospheric Rossby wave (Ding et al. 2011; Nicolas and Bromwich 2014). Increasing sea surface temperatures (SSTs) in the western tropical Pacific result in the cyclonic anomalies in the Weddell Sea, which cause warming in the South Pole and cooling in the Antarctic Peninsula (Clem et al. 2019, 2020). The pattern of SST in the tropical Pacific Ocean has changed, with negative SST anomalies in the equatorial eastern tropical Pacific since the end of the twentieth century, as shown by the negative phase of the interdecadal Pacific oscillation (IPO). Due to the similar spatial patterns of SST anomalies to ESNO, the IPO is also considered as the ENSO-like decadal variability. Thus, to a certain extent, IPO arises as a residual of largely independent ENSO events (Newman et al. 2016; Power et al. 2021). Its changes or phrase transition has been shown to modulate the ENSO teleconnection at the interannual scale (Dong et al. 2018). There still exists question concerning the cooling over the West Antarctica is primarily attributable to what processes and mechanisms and from which areas.

Data and methods

In this study, we used the monthly mean surface atmospheric temperature (SAT; measured at 2 m above ground) data at Byrd Station by Bromwich et al. (2013, 2014), which is the only WAIS station with complete long-term temperature records from 1958 to 2021. Their annual and seasonal averages show high and significant correlations ($r > 0.8$, $p < 0.05$) with ERA5 temperature fields over most of the WAIS (Figs. 1g–k), which reveals the robustly
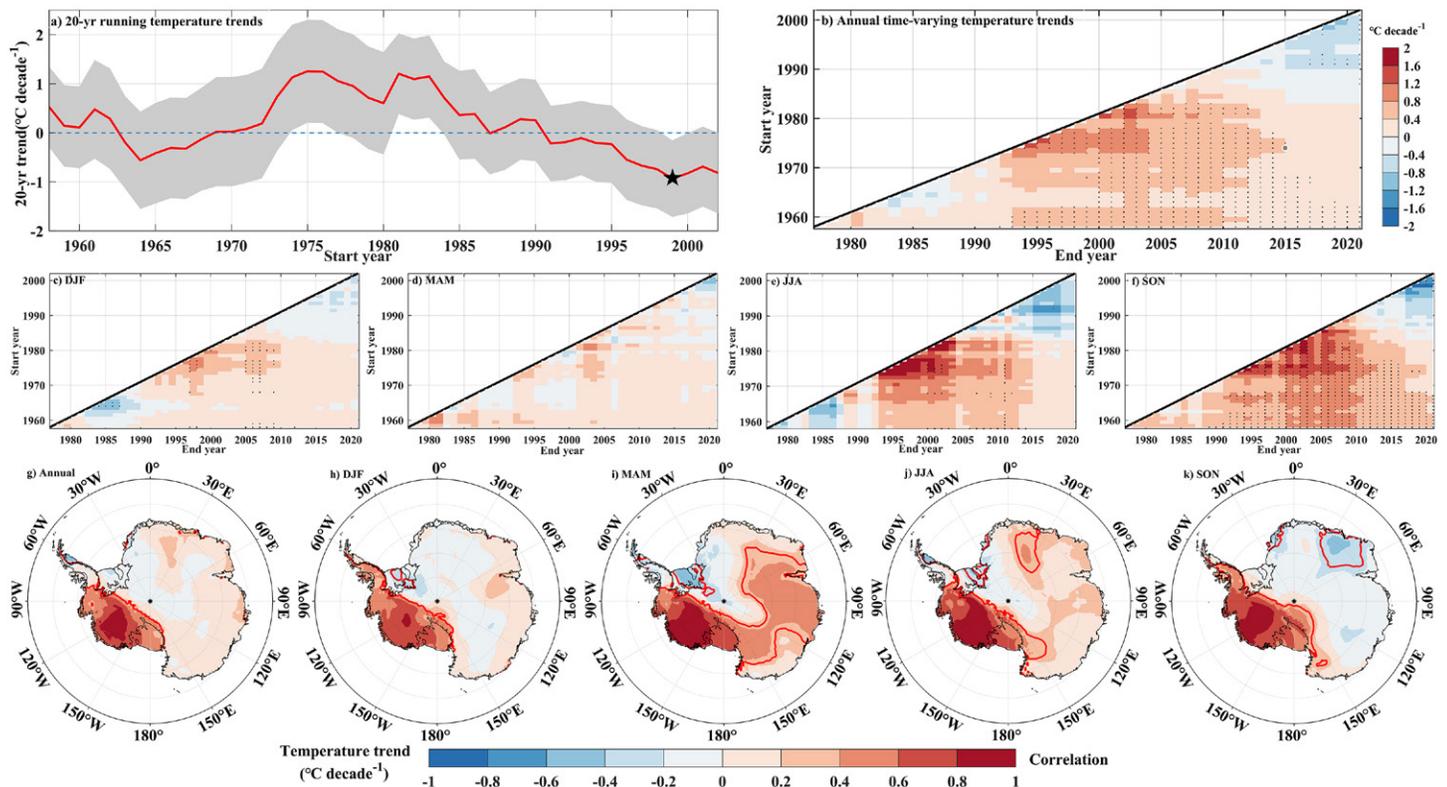
Fig. 1. (a)–(f) Surface air temperature (SAT) changes at the Byrd Station during 1958–2021. (a) Running 20-yr SAT trends (°C decade⁻¹) at the start of the trend period, with the *p* < 0.05 confidence interval shaded in gray. The strongest significant cooling from 1999 to 2018 is labeled by pentagram. (b)–(f) The time-varying annual and seasonal mean SAT trends, with *p* < 0.05 indicated by stippling: (b) annual, (c) December–February (DJF), (d) March–May (MAM), (e) June–August (JJA), and (f) September–November (SON). (g)–(k) The correlation of annual and seasonal averaged SAT with ERA5 during 1979–2021, region with *p* < 0.05 outlined by red lines: (g) annual, (h) DJF, (i) MAM, (j) JJA, (k) SON. In (b)–(f), the *y* axis is the start year of the trend, and the *x* axis is the end year of the trend; the *x* = *y* axis is exactly the 20-yr trend, and the periods exceeding 20-yr are in the lower-right half.

representative for the central WAIS, and this is also confirmed by Bromwich et al. (2013, 2014). We utilized the monthly mean ERA5 fields, including sea level pressure (SLP), 850 hPa geopotential heights (Z850), and 850 hPa wind. Averaged SST data are derived from the NOAA Extended Reconstructed Sea Surface Temperature (SST) V5 (ERSSTv.5). The monthly mean sea ice concentration (SIC) data come from the NOAA/NSIDC Climate Data Record of Passive Microwave Sea Ice Concentration, version 4. The IPO changes was quantified by the unfiltered tripole index from NOAA ERSSTv.5. We use the station-based index of the Southern Annular Mode (SAM) by Marshall (2003). Given the availability of the monthly mean oceanic and atmospheric fields, our analysis is focused on the 1979–2018 interval. The standard least squares linear regression, correlation analysis and linear congruency are applied to explore SAT changes, the regional atmospheric circulation trends, and their linkages with tropical climate variability. The statistical significance was assessed via the Student's *t* test. We applied the empirical orthogonal function (EOF) to examine the annual and seasonal sea level pressure (SLP) variability from 40° to 90°S, to identify the main modes of SLP changes. EOF analysis is a variance-maximizing multivariate statistical technique, which supports the hypothesis that regional atmospheric circulation changes are related to SST variability in the tropical Pacific. To capture the dominant coupled modes of variation between the tropical Pacific SST and the regional scale climate variability, the potential connections between the Southern Hemisphere Z850 (60°–90°S) and SST variability were determined by maximum covariance analysis (MCA).

Results

Recent cooling trends on the WAIS.

The time series of running 20-yr (Fig. 1a) and the time-varying (Fig. 1b) trends of annual mean SAT at Byrd Station exhibit sustainable cooling from the early 1990s onward. In particular, the epoch from 1999 to 2018 experienced the largest 20-yr box window decrease of the annual mean SAT, at a rate of −0.93°C decade^{-1} ($p < 0.05$). The seasonal mean SAT also decreased for the same time interval (1999–2018) (Figs. 1c–f). The spring cooling was strongest at about twice the annual mean trend (−1.84°C decade^{-1}), and winter ranked second strongest (−1.19°C decade^{-1}), with the very weak cooling in autumn and summer. However, for the four seasons, only the spring 20-yr box windowed cooling was statistically significant at the confidence level of $p < 0.05$. These cooling trends derived from our in situ measurements are consistent with those determined by MODIS land surface temperature products and ERA5 (Figs. ES1 and ES2 in the online supplemental material). Despite the different magnitudes of cooling among databases, they share a common cooling in winter, spring, and annual mean across the region centered at the WAIS Marie Byrd Land sector.

Atmospheric circulation and sea ice changes on and around Antarctica.

EOF analysis is used to identify the leading modes of annual and seasonal mean SLP variability during 1999–2018 (Fig. 2). We only analyze the spatial patterns and time series (PCs) of the first two EOF modes (EOF1 and EOF2) and their related large-scale circulation states. The EOF1
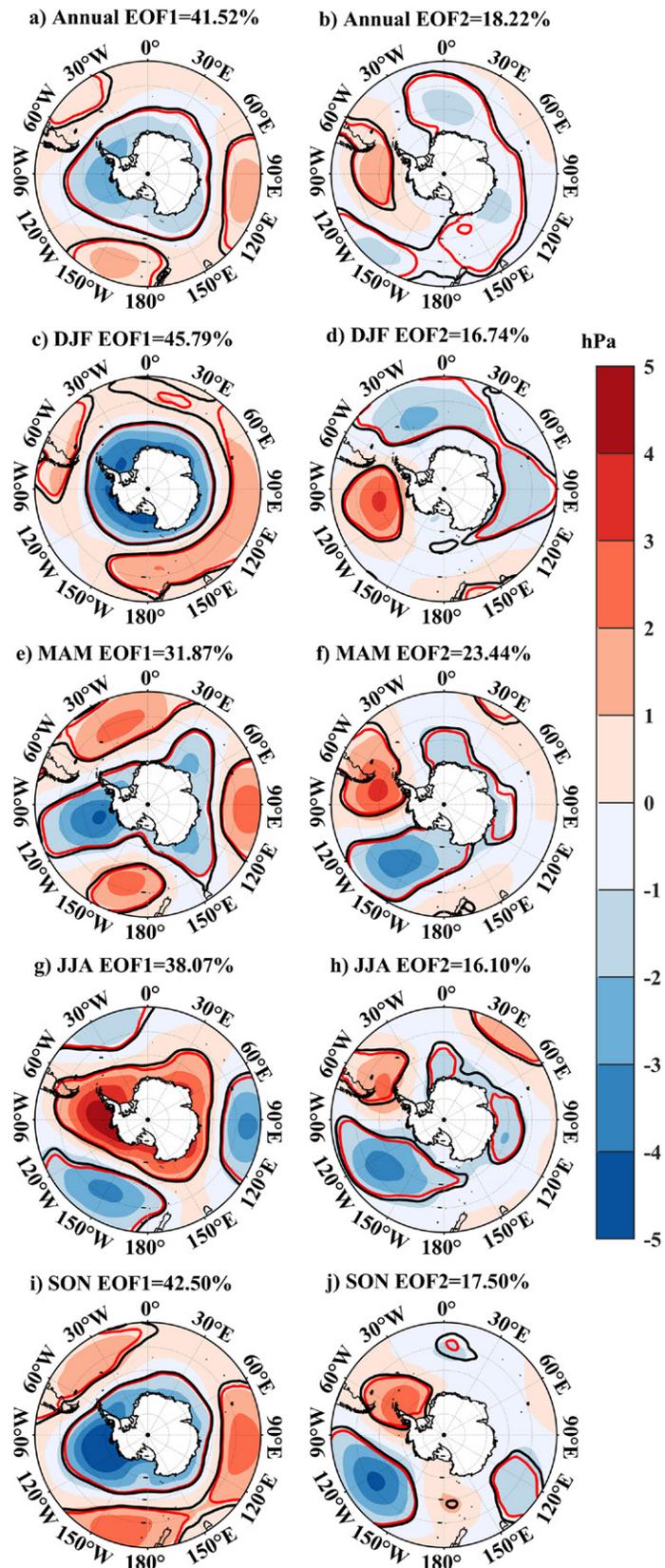

Fig. 2. Principal modes of annual and seasonal SLP. EOF analysis associated with the first two EOF modes for 1999–2018 on the SLP. The amplitude of each EOF is regressed onto SLP to indicate the variability of SLP associated with the principal component. The percentage shown in the top center of each subplot lists the amount of variance associated with which each EOF. The black and red lines outline the areas significant at the confidence levels of $p < 0.1$ and $p < 0.05$, respectively.

explains approximately 31%–46% of the variance of annual and seasonal mean SLP, and represents the atmospheric circulation anomalies resembling the SAM pattern. In particular, the circulation anomalies near the Amundsen Sea low (ASL) are the most prominent feature of atmospheric circulation of the EOF1 for annual and spring SLP. Preceding studies highlight the cooling effect associated with the SAM positive polarity for West Antarctica, especially in austral summer and autumn (Marshall 2007; Nicolas and Bromwich 2014; Marshall and Thompson 2016; Jones et al. 2019; Fogt and Marshall 2020). However, there is no significant correlations between observed SAM index by Marshall (2003) and SATs in summer during 1999–2018 (Fig. ES3). Furthermore, the weak negative correlations show the limited contribution of SAM to West Antarctic cooling of autumn air temperature. Despite the significantly negative correlation of winter SATs with SAM, no marked SAM positive polarity occurred in winter.

EOF2 captures about 16%–24% of the variability of annual and seasonal SLP. In annual mean, EOF2 consists of the anomalous cyclones near the Weddell Sea and South Indian and Pacific Oceans, and anticyclone near the Drake Passage. Summer EOF2 is mainly composed of high SLP system over the Bellingshausen and Amundsen Seas and low SLP system over the Weddell Sea and south Indian Ocean, which correspond to the circulation conditions that promote the cooling of the Antarctic Peninsula (Randel and Wu 1999; Turner et al. 2016; Jones et al. 2019). In autumn, the EOF2 spatial pattern shows a dipole structure between the Drake Passage (high pressure anomalies) and the Ross Sea (low pressure anomalies). In winter and spring, the EOF2 patterns exhibit significant negative SLP anomalies move westward to the Amundsen Sea, which is indicative of a classic stationary Rossby wave response to tropical SST forcing (Maclennan and Lenaerts 2021). We find a statistically significant and positive correlation between EOF2 principal component time series (PC2) in spring with the corresponding West Antarctic air temperature ($r = 0.61$, $p < 0.05$, Fig. 3). In September–November (SON), the EOF2 consists of significantly negative SLP anomalies over the eastern Amundsen Sea (Maclennan and Lenaerts 2021), and a blocking high in the Drake Passage and northern Antarctic Peninsula, which resembles with the Pacific–South American mode 1 (PAS1), related to the SST anomalies on the tropical Pacific Ocean. The cyclonic conditions in the Amundsen Sea from a low pressure system and anticyclone in the Drake Passage and in the northern Antarctic Peninsula from a high pressure system promote the prevalence of cold and dry southwesterly wind over the continental WAIS (Fig. 4), causing the temperature decreasing trend. In summer, the positive sea ice concentration (SIC) trend for the 1999–2018 period (Fig. 4) over the Weddell Sea amplifies the effects of the cyclonic conditions on the cooling on the Antarctic Peninsula (Turner et al. 2016). SIC in the Amundsen Sea showed a significant increase during JJA and SON (Fig. 4) due to the offshore airflow along the WAIS coasts caused by the winds from the Weddell Sea, which in turn helps to enhance the cooling effects on this region.

Tropical teleconnection with Antarctic atmospheric circulation variability. Previous works have demonstrated that the ENSO forcing from the tropical Pacific influences WAIS climate by forcing interannual changes in the position and intensity of the ASL (Clem et al. 2017; Deb et al. 2018). The atmospheric circulation changes over the Amundsen Sea, causing WAIS winter warming from the 1950s to the 2000s, which is closely related to the SST increase in the central tropical Pacific Ocean (Ding et al. 2011). However, since the late 1990s, SST in the tropical Pacific varies. For the 1999–2018 period, the annual and all seasonal SST in the western tropical Pacific exceeded those for 1979–97, while the SST in the central and east Pacific was lower, and differences are significant ($p < 0.05$) (Fig. 5). The large regional differences of the SST in the tropical Pacific indicates the significant negative phase of the IPO (Fig. 6), and thus a relatively strong polar front jet (PFJ), as
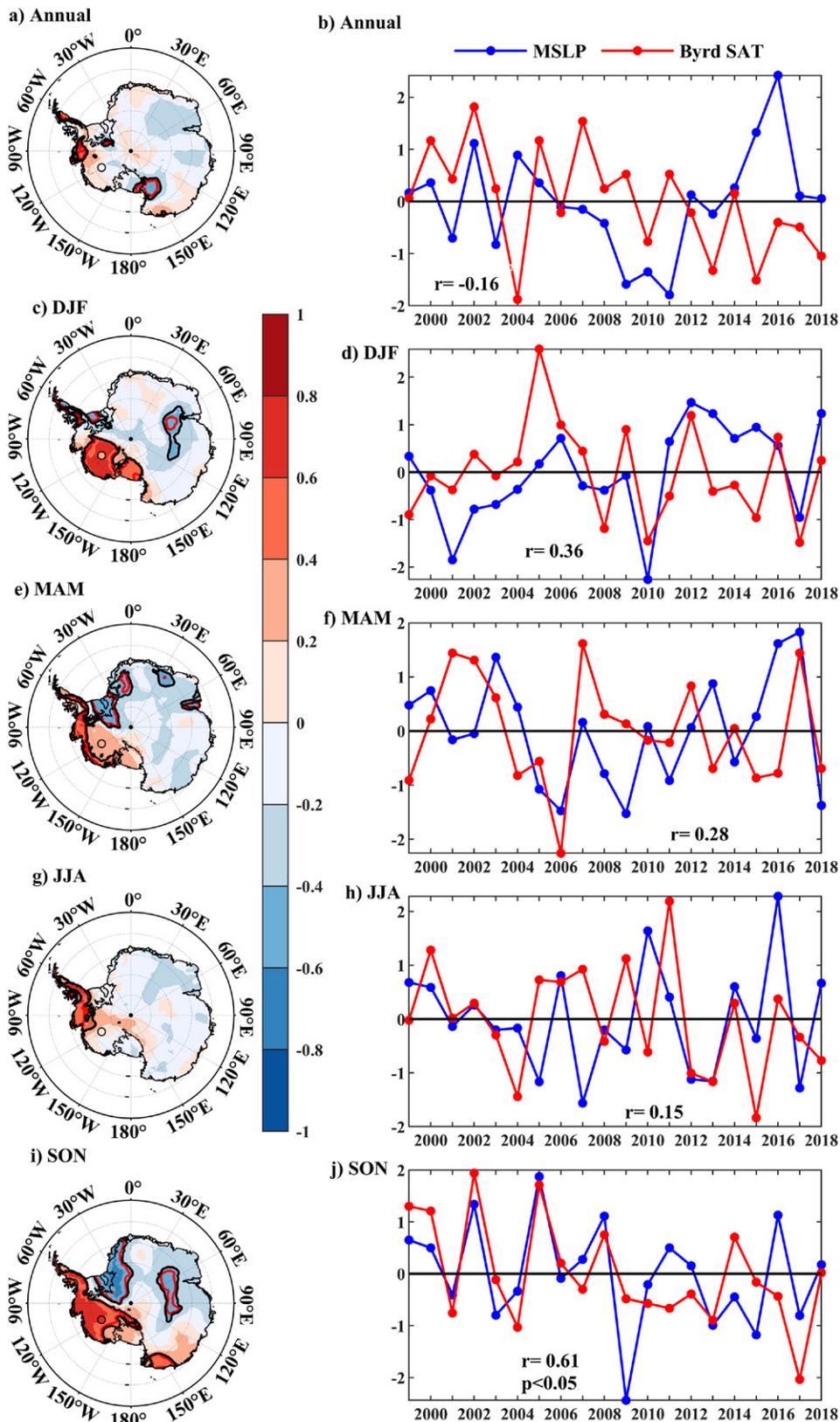
Fig. 3. (left) Correlations between the time series of the second empirical orthogonal function mode (PC2) with ERA5 SAT (panel) and Byrd SAT (circle). (right) The time series of the PC2 and Byrd SAT. The black and red lines outline the areas significant at the confidence levels of $p < 0.1$ and $p < 0.05$, respectively.

previously reported by Trenberth et al. (2014). This leads to an anomalous descent generated over the central to eastern tropical Pacific, and an anomalous ascent in the tropical western Pacific, with strengthening of the Walker circulation (Clem and Fogt 2015).
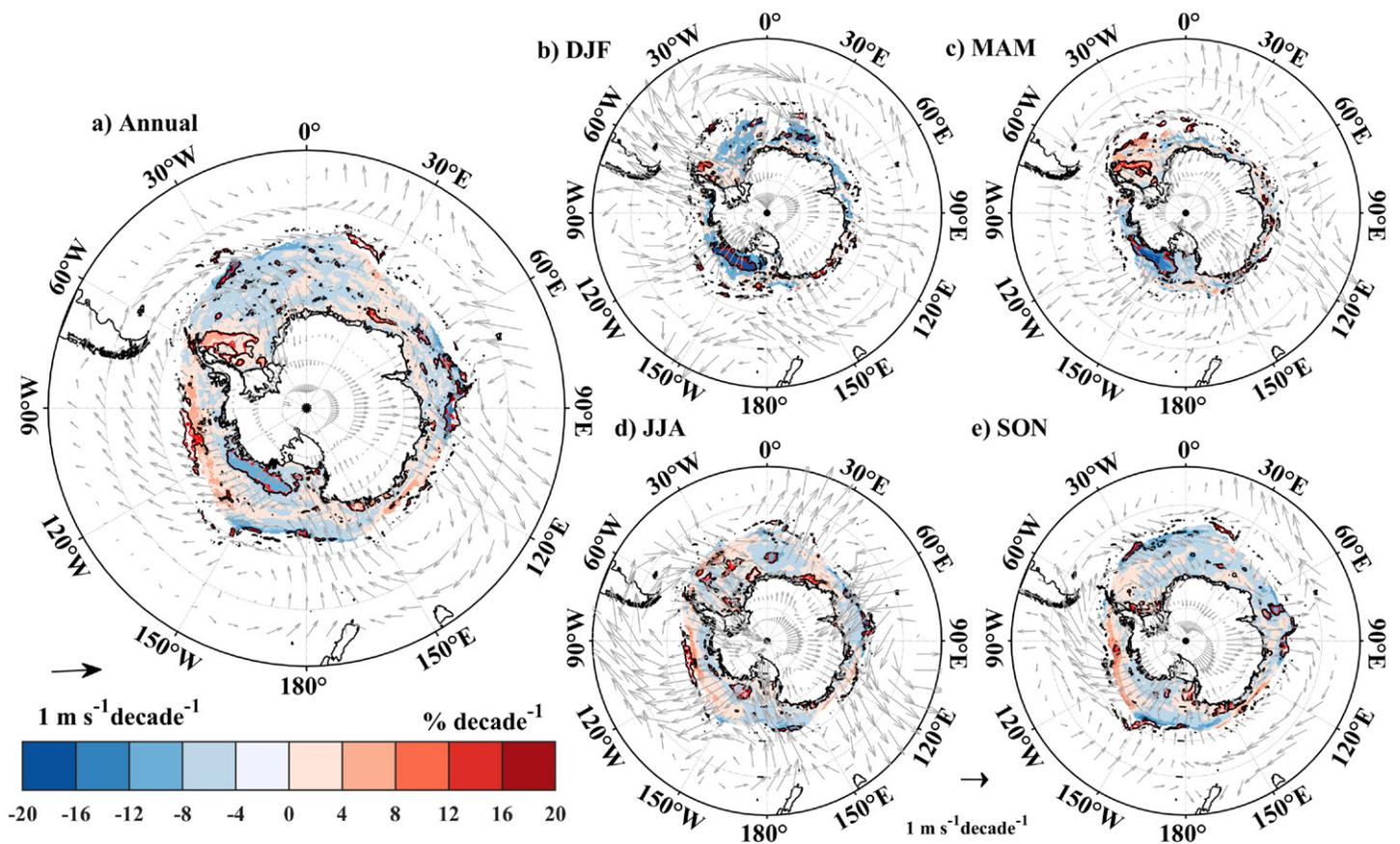
Fig. 4. Annual and seasonal mean trends in oceanic and atmospheric conditions from 1999 to 2018, including SIC and 850 hPa wind. The black and red lines outline the areas significant at the confidence levels of $p < 0.1$ and $p < 0.05$, respectively.

The negative SST anomalies in the tropical central Pacific and the corresponding convection and high-level vorticity changes trigger the quasi-stationary Rossby wave trains. The latter are similar to those observed during a La Niña event, which propagate from the tropics along a great-circle trajectory through the South Pacific (Clem and Fogt 2015; Turner et al. 2016) to high latitudes. The response of anomalous Rossby wave activity is modulated by westerly changes as well as the mean zonal circulation, which lead to regional atmospheric circulation anomalies over the southern polar region (Li et al. 2021). The IPO is an ENSO-like decadal variability on the both sides of the tropical Pacific basin. IPO index and Niño-3.4 index exhibit very similar interannual variability (Fig. 6). It is of vital importance to find a method to separate signals of IPO from ENSO. Because the IPO arises as a residual of largely independent ENSO events, associated with the low-frequency modulation of ENSO (Newman et al. 2016; Power et al. 2021), a viable alternative to determine the separate signals is to remove covariability with Niño-3.4 SSTs from the IPO index by means of a linear regression approach (Clem et al. 2020; Fig. 6). Relative to the raw IPO index, the IPO residual index can better represent the phase of the IPO as presented by the low-pass-filtered IPO index, which uses the Chebyshev filter with a cutoff period of 13 years and a filter order of 6 (Henley et al. 2015; Fig. 6). To explore the effect of the IPO on atmospheric circulation variability on and around Antarctica, first, our strategy is to calculate the linear congruency of the IPO with SLP. The SLP fields are regressed onto the IPO residual index, and then the regression coefficient of each grid cell is multiplied by the observed trend in the IPO residual index (Fig. 7). Second, we employ maximum covariance analysis (MCA) of seasonal means of tropical SST and Z850 for the 1999–2018 period (Figs. ES3 and ES4). Third, the SLP PC2 time series are linearly regressed by the SST changes (Fig. 8).
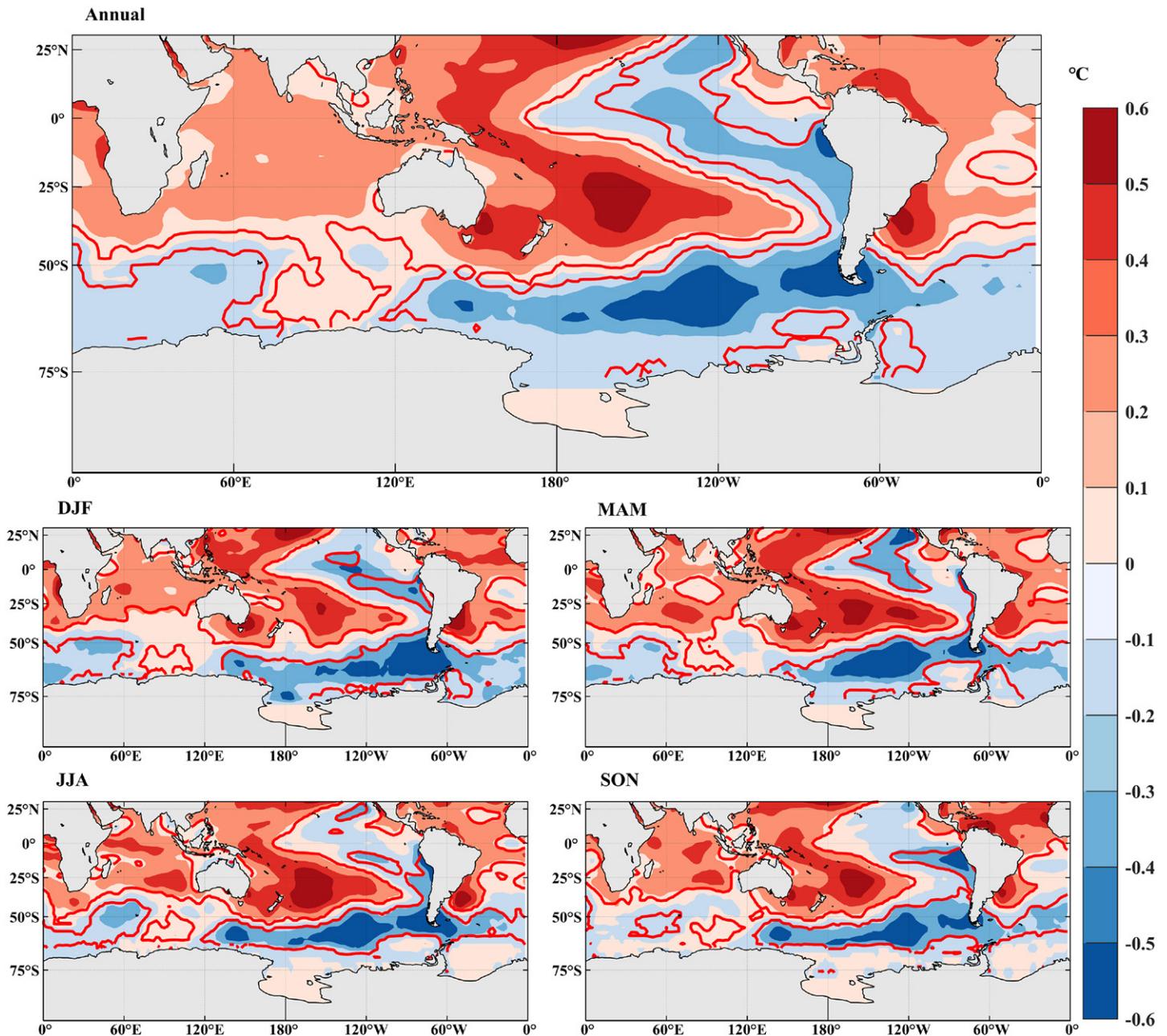
Fig. 5. Difference in mean SST between 1999–2018 and 1979–98. The red contours outline areas of differences that are statistically significant at the $p < 0.05$ confidence level.

The decrease in SLP over the Amundsen Sea is linearly congruent with the negative trend of IPO (Fig. 7), in agreement with the previous studies (Turner et al. 2016; Clem et al. 2020) that the negative phase of the IPO from the late 1990s onward contribute much of the negative SLP anomalies in the ASL region and the Weddell Sea. MCA results consist of pairs of spatial modes and corresponding time series, representing covarying tropical SST and Z850 structures (Figs. ES3 and ES4). For the two fields analyzed here, the tropical SST mode can be physically interpreted as the forcing, and the Z850 mode as the response. Leading pairs of MCA patterns thus indicate those patterns of tropical SST anomalies that most strongly influence the Southern Hemisphere extratropical circulation. The strongest SST signal is a cooling in the central and eastern Pacific, which then gives to the negative trends of Z850 in the ASL region, especially, in SON during 1999–2018. In addition, regressions of SST onto the PC2 time series show that the SON atmospheric circulation explained by EOF2 is robustly associated with the IPO-related SST anomalies (Fig. 8). The negative phase of IPO
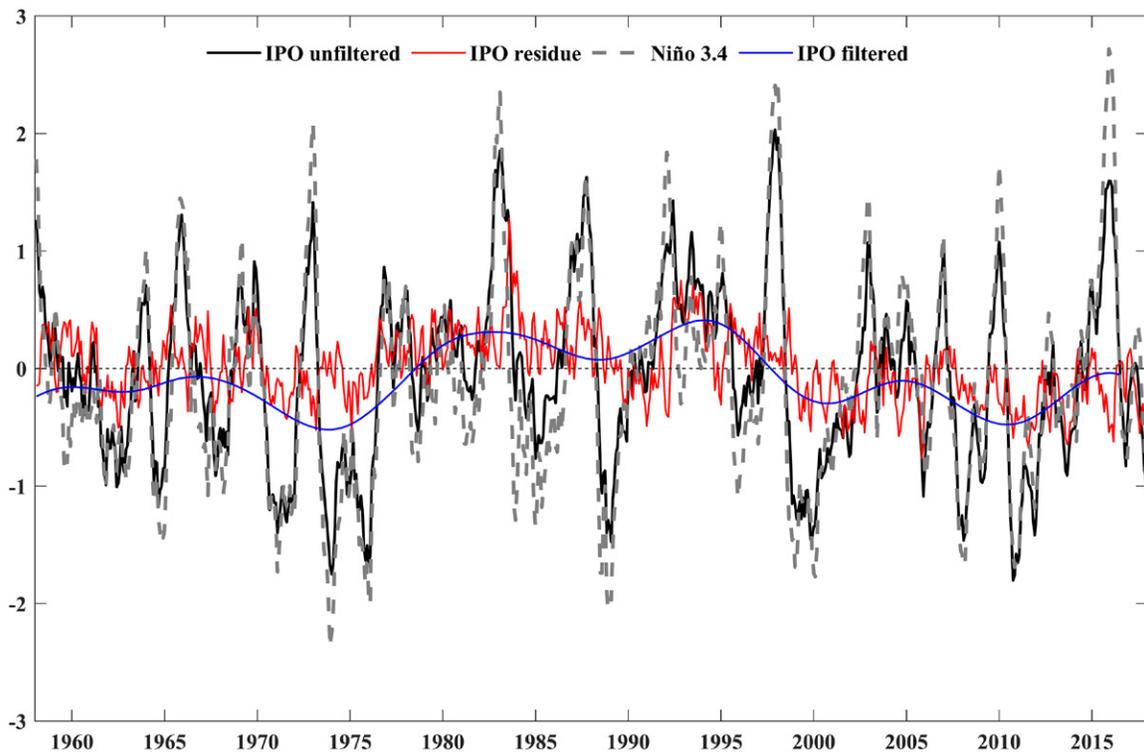
Fig. 6. The monthly mean IPO unfiltered index, IPO filtered index, IPO residual index, and Niño-3.4 index.

causes cyclonic anomalies in the eastern ASL region (Figs. 2 and 8) through the transmission of Rossby wave trains. This teleconnection to the high-latitude South Pacific increases the pressure gradient and enhances the southerly flow along the westward flank of the cyclone (Fig. 4), decreasing the SATs over the continental central WAIS. In austral spring when negative IPO is more intense, the subtropical jet stream is stronger, and is centered where it can act as a waveguide (Li et al. 2021).

Discussion and conclusions

The absence of West Antarctic warming in the early twenty-first century is reminiscent of the event of global mean SAT slowdown (global warming hiatus), with the negative phase of the IPO being one of their common major possible causes. The global warming hiatus ended during the early 2010s, and warming reaccelerated associated with the shift of the Pacific decadal oscillation (PDO) from negative phase to positive phase, the increasing North Atlantic Oscillation (NAO), and the positive phase of Atlantic multidecadal oscillation (AMO) (Zhang et al. 2019). However, cooling over the WAIS still appeared over the early 2010s, suggesting the West Antarctic climate is more sensitive to tropical Pacific forcing, compared to PDO, NAO, and AMO. A recent study (Li et al. 2021) also reported that a teleconnection pattern may be established by the tropical Atlantic and Indian Oceans, driving the Rossby wave trains through direct and indirect paths, and affecting the SAT change of the WAIS, but the effect is relatively weak.

In conclusion, the WAIS experienced a significant cooling trend, especially in spring, during the recent 20 years (1999–2018), which is a response to the interactions of coupled sea ice, ocean, and atmosphere. Here we attributed the observed significant spring cooling to the strong cyclonic anomalies in the Amundsen Sea, and anticyclonic conditions in the Drake Passage and Antarctic Peninsula presented by EOF2, related to negative IPO, and the increase of SIC in the Amundsen Sea also driven by tropical forcing. While the cooling effect of the positive SAM on West Antarctica is expected (Marshall 2007; Marshall and Thompson 2016; Fogt and Marshall 2020), it has not played a role in the recent cooling. This underscores the
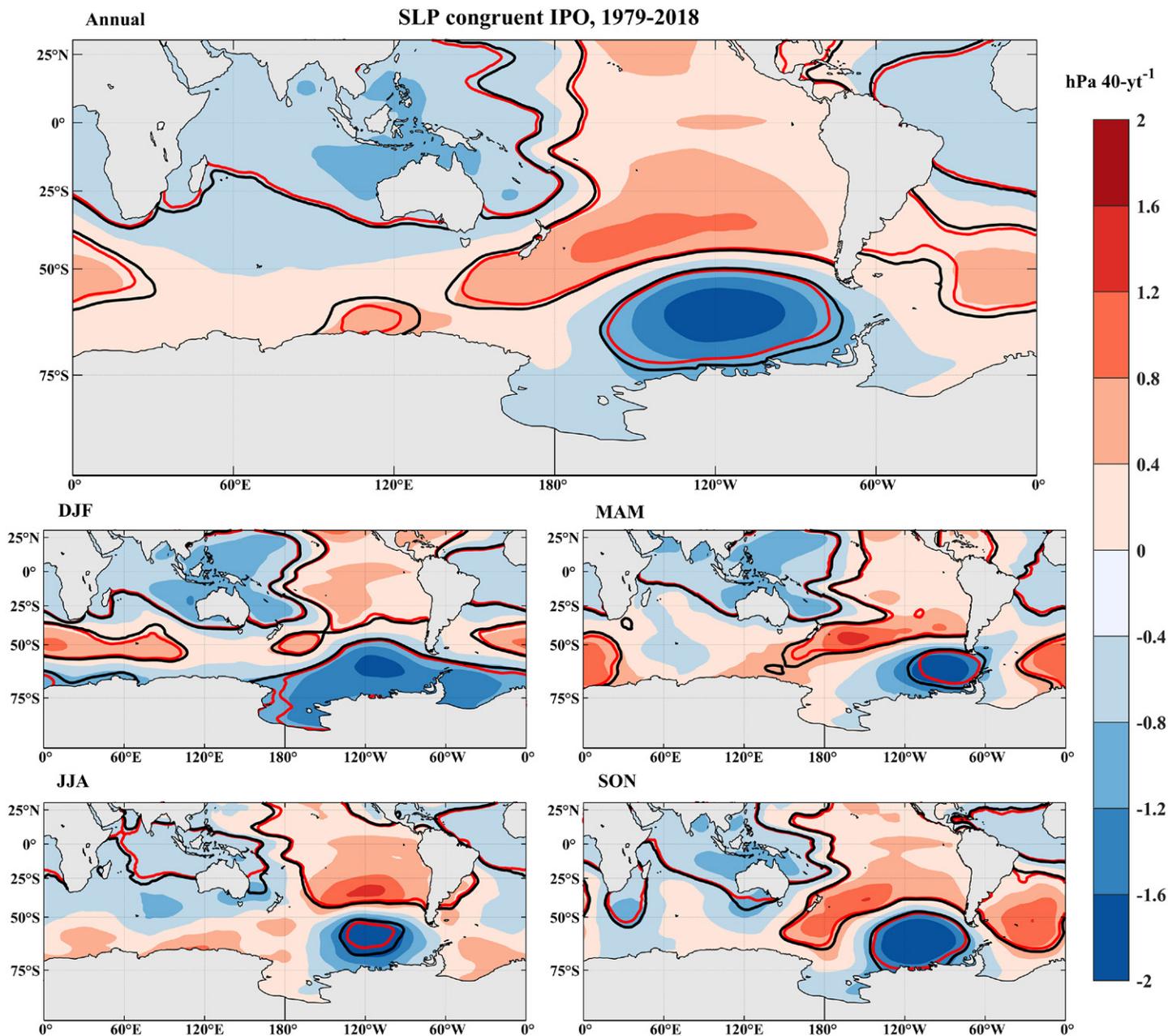
Fig. 7. Trends in annual and seasonal SLP linearly congruent with negative IPO residual index in 1979–2018. The black and red contours outline the areas of correlations, trends, and differences, significant at the confidence levels of $p < 0.1$ and $p < 0.05$, respectively.

importance of regional atmospheric circulation variability associated with the tropical Pacific SST anomalies for driving the central WAIS air temperature. There is no robust agreement on the tropical Pacific SST variability in the future by the different atmospheric global climate models (AGCMs) (Lee et al. 2021). However, Cai et al. (2022) show a robust increase of the projected change in ENSO-related SST variability under all emission scenarios when applied over a century-long time window, IPO variability has not been fully explored for future projections. Thus, this confirms that the tropical Pacific climate oscillation is still an important source of uncertainty in West Antarctic air temperature obtained from future projections.

The GCMs from the phase 6 of the Coupled Model Intercomparison Project (CMIP6) are an important tool to make the projections of future climate changes over Antarctica. However, 28 CMIP6 multimodel ensemble mean in historical does not capture the significant cooling trend of the WAIS over the early twenty-first century, but the significant warming trend at the South Pole reported by Clem et al. (2020) (Fig. ES6, Table ES1), which implies substantial
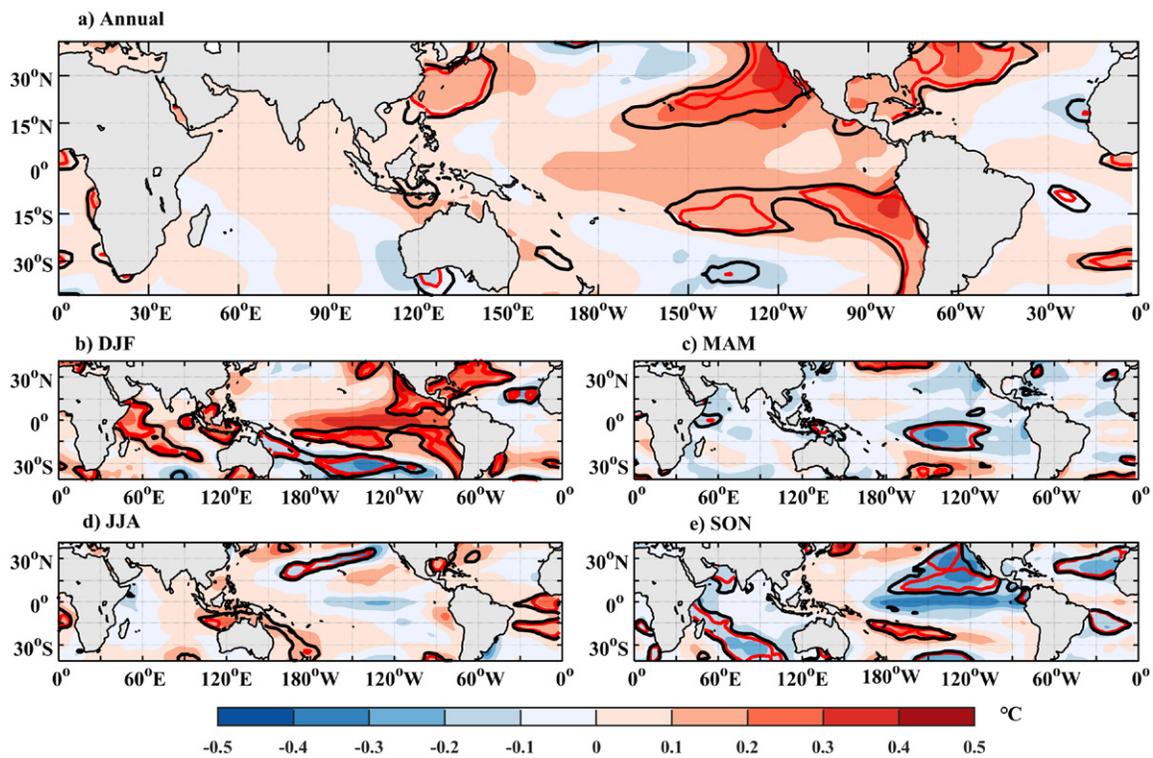
Fig. 8. The sea surface temperature regressed to the time series of the second empirical orthogonal function mode (PC2) of annual and seasonal SLP from 1999 to 2018. The black and red lines outline the areas with trends significant at $p < 0.1$ and $p < 0.05$ confidence interval, respectively.

uncertainties in the future temperature projections of CMIP6 models on the WAIS. It is easy to understand that, despite the relatively high reliability of the models for the global-scale temperature changes, their representations of climatological interdecadal transitions over Antarctica are generally less accurate, probably due to their coarse resolution and sparseness of polar-special physical schemes. Therefore, for the better projections of future Antarctic temperature changes, the GCMs cannot ignore the influence of the interdecadal oscillation and need to incorporate more physical mechanisms.

Data availability statement. The monthly mean SAT data for Byrd Station are available from https://polarmet.osu.edu/datasets/Byrd_recon/. ERA5 data are provided by the European Centre for Medium-Range Weather Forecasts (ECMWF) (https://cds.climate.copernicus.eu/cdsapp#!/search?type=dataset). IPO indices can be freely available at (https://psl.noaa.gov/data/timeseries/IPOTPI/). Averaged SST data are obtained from NOAA (https://psl.noaa.gov/data/gridded/data.noaa.ersst.v5.html). SIC data are available from the National Snow and Ice Data Center (NSIDC) (https://nsidc.org/data/G02202/versions/4). SAM index data come from British Antarctic Survey (http://www.nerc-bas.ac.uk/icd/gjma/sam.html).

References

Bromwich, D. H., J. P. Nicolas, A. J. Monaghan, M. A. Lazzara, L. M. Keller, G. A. Weidner, and A. B. Wilson, 2013: Central West Antarctica among the most rapidly warming regions on Earth. *Nat. Geosci.*, **6**, 139–145, https://doi.org/10.1038/ngeo1671.

——, ——, ——, ——, ——, ——, and ——, 2014: Correction: Corrigendum: Central West Antarctica among the most rapidly warming regions on Earth. *Nat. Geosci.*, **7**, 76, https://doi.org/10.1038/ngeo2016.

Cai, W., B. Ng, G. Wang, A. Santoso, L. Wu, and K. Yang, 2022: Increased ENSO sea surface temperature variability under four IPCC emission scenarios. *Nat. Climate Change*, **12**, 228–231, https://doi.org/10.1038/s41558-022-01282-z.

Clem, K. R., and R. L. Fogt, 2015: South Pacific circulation changes and their connection to the tropics and regional Antarctic warming in austral spring, 1979–2012. *J. Geophys. Res. Atmos.*, **120**, 2773–2792, https://doi.org/10.1002/2014JD022940.

——, J. A. Renwick, and J. McGregor, 2017: Large-scale forcing of the Amundsen Sea low and its influence on sea ice and West Antarctic temperature. *J. Climate*, **30**, 8405–8424, https://doi.org/10.1175/JCLI-D-16-0891.1.

——, B. R. Lintner, A. J. Broccoli, and J. R. Miller, 2019: Role of the South Pacific convergence zone in West Antarctic decadal climate variability. *Geophys. Res. Lett.*, **46**, 6900–6909, https://doi.org/10.1029/2019GL082108.

——, R. L. Fogt, J. Turner, B. R. Lintner, G. J. Marshall, J. R. Miller, and J. A. Renwick, 2020: Record warming at the South Pole during the past three decades. *Nat. Climate Change*, **10**, 762–770, https://doi.org/10.1038/s41558-020-0815-z.

Deb, P., A. Orr, D. H. Bromwich, J. P. Nicolas, J. Turner, and J. S. Hosking, 2018: Summer drivers of atmospheric variability affecting ice shelf thinning in the Amundsen Sea Embayment, West Antarctica. *Geophys. Res. Lett.*, **45**, 4124–4133, https://doi.org/10.1029/2018GL077092.

Ding, Q., E. J. Steig, D. S. Battisti, and M. Küttel, 2011: Winter warming in West Antarctica caused by central tropical Pacific warming. *Nat. Geosci.*, **4**, 398–403, https://doi.org/10.1038/ngeo1129.

Dong, B., A. Dai, M. Vuille, and O. E. Timm, 2018: Asymmetric modulation of ENSO teleconnections by the interdecadal Pacific oscillation. *J. Climate*, **31**, 7337–7361, https://doi.org/10.1175/JCLI-D-17-0663.1.

Fogt, R. L., and G. J. Marshall, 2020: The Southern Annular Mode: Variability, trends, and climate impacts across the Southern Hemisphere. *Wiley Interdiscip. Rev.: Climate Change*, **11**, e652, https://doi.org/10.1002/wcc.652.

Henley, B. J., J. Gergis, D. J. Karoly, S. Power, J. Kennedy, and C. K. Folland, 2015: A tripole index for the interdecadal Pacific oscillation. *Climate Dyn.*, **45**, 3077–3090, https://doi.org/10.1007/s00382-015-2525-1.

Jones, M. E., D. H. Bromwich, J. P. Nicolas, J. Carrasco, E. Plavcová, X. Zou, and S. H. Wang, 2019: Sixty years of widespread warming in the southern middle and high latitudes (1957–2016). *J. Climate*, **20**, 6875–6898, https://doi.org/10.1175/JCLI-D-18-0565.1.

Kimura, S., and Coauthors, 2017: Oceanographic controls on the variability of ice-shelf basal melting and circulation of glacial meltwater in the Amundsen Sea Embayment, Antarctica. *J. Geophys. Res. Oceans*, **122**, 10131–10155, https://doi.org/10.1002/2017JC012926.

Lee, J. Y., and Coauthors, 2021: Future global climate: Scenario-based projections and near-term information. *Climate Change 2021: The Physical Science Basis*, V. Masson-Delmotte et al., Eds., Cambridge University Press, 1–195.

Lenton, T. M., 2021: Tipping points in the climate system. *Weather*, **76**, 325–326, https://doi.org/10.1002/wea.4058.

Li, X., and Coauthors, 2021: Tropical teleconnection impacts on Antarctic climate changes. *Nat. Rev. Earth Environ.*, **2**, 680–698, https://doi.org/10.1038/s43017-021-00204-5.

Maclennan, M. L., and Lenaerts, J. T. M., 2021: Large-scale atmospheric drivers of snowfall over Thwaites Glacier, Antarctica. *Geophys. Res. Lett.*, **48**, e2021GL093644, https://doi.org/10.1029/2021GL093644.

Marshall, G. J., 2003: Trends in the Southern Annular Mode from observations and reanalyses. *J. Climate*, **16**, 4134–4143, https://doi.org/10.1175/1520-0442(2003)016<4134:TITSAM>2.0.CO;2.

——, 2007: Half-century seasonal relationships between the Southern Annular Mode and Antarctic temperatures. *Int. J. Climatol.*, **27**, 373–383, https://doi.org/10.1002/joc.1407.

——, and D. W. J. Thompson, 2016: The signatures of large-scale patterns of atmospheric variability in Antarctic surface temperatures. *J. Geophys. Res. Atmos.*, **121**, 3276–3289, https://doi.org/10.1002/2015JD024665.

Newman, M., and Coauthors, 2016: The Pacific decadal oscillation, revisited. *J. Climate*, **29**, 4399–4427, https://doi.org/10.1175/JCLI-D-15-0508.1.

Nicolas, J. P., and D. H. Bromwich, 2014: New reconstruction of Antarctic near-surface temperatures: Multidecadal trends and reliability of global reanalyses. *J. Climate*, **27**, 8070–8093, https://doi.org/10.1175/JCLI-D-13-00733.1.

Power, S., and Coauthors, 2021: Decadal climate variability in the tropical Pacific: Characteristics, causes, predictability and prospects. *Science*, **374**, eaay9165, https://doi.org/10.1126/science.aay9165.

Randel, W. J., and F. Wu, 1999: Cooling of the Arctic and Antarctic polar stratospheres due to ozone depletion. *J. Climate*, **12**, 1467–1479, https://doi.org/10.1175/1520-0442(1999)012<1467:COTAAA>2.0.CO;2.

Rignot, E., J. Mouginot, B. Scheuchl, and M. Morlighem, 2019: Four decades of Antarctic Ice Sheet mass balance from 1979–2017. *Proc. Natl. Acad. Sci. USA*, **116**, 1095–1103, https://doi.org/10.1073/pnas.1812883116.

Schellnhuber, H. J., 2009: Tipping elements in the Earth system. *Proc. Natl. Acad. Sci. USA*, **106**, 20561–20563, https://doi.org/10.1073/pnas.0911106106.

Steig, E. J., D. P. Schneider, S. D. Rutherford, M. E. Mann, J. C. Comiso, and D. T. Shindell, 2009: Warming of the Antarctic ice-sheet surface since the 1957 International Geophysical Year. *Nature*, **457**, 459–462, https://doi.org/10.1038/nature07669.

Trenberth, K. E., J. T. Fasullo, G. Branstator, and A. S. Phillips, 2014: Seasonal aspects of the recent pause in surface warming. *Nat. Climate Change*, **4**, 911–916, https://doi.org/10.1038/nclimate2341.

Turner, J., H. Lu, I. White, J. C. King, T. Phillips, J. S. Hosking, and P. Deb, 2016: Absence of 21st century warming on Antarctic Peninsula consistent with natural variability. *Nature*, **535**, 411–415, https://doi.org/10.1038/nature18645.

Zhang, C., S. Li, F. Luo, and Z. Huang, 2019: The global warming hiatus has faded away: An analysis of 2014–2016 global surface air temperatures. *Int. J. Climatol.*, **39**, 4853–4868, https://doi.org/10.1002/joc.6114.